^{18}O-Exchange Evidence That Mutations of Arginine in a Signature Sequence for P-Type Pumps Affect Inorganic Phosphate Binding†

Robert A. Farley,‡,§ Emad Elquza,‡ Jochen Müller-Ehmsen,‡ David J. Kane,‡,|| Agnes K. Nagy,|| Vladimir N. Kasho,|| and Larry D. Faller*,||,⊥

Department of Physiology and Biophysics and Department of Biochemistry and Molecular Biology, University of Southern California School of Medicine, Los Angeles, California 90033, and CURE: Digestive Diseases Research Center, Department of Medicine, School of Medicine, and Department of Physiological Sciences, University of California at Los Angeles, and Veterans Administration Greater Los Angeles Health Care System, Los Angeles, California 90073

Received February 7, 2001; Revised Manuscript Received March 26, 2001

ABSTRACT: We have proposed a model for part of the catalytic site of P-type pumps in which arginine in a signature sequence functions like lysine in P-loop-containing enzymes that catalyze adenosine 5′-triphosphate hydrolysis [Smirnova, I. N., Kasho, V. N., and Faller, L. D. (1998) *FEBS Lett. 431*, 309−314]. The model originated with evidence from site-directed mutagenesis that aspartic acid in the DPPR sequence of Na,K-ATPase binds Mg^{2+} [Farley, R. A., et al. (1997) *Biochemistry 36*, 941−951]. It was developed by assuming that the catalytic domain of P-type pumps evolved from enzymes that catalyze phosphoryl group transfer. The functions of the positively charged amino group in P-loops are to bind substrate and to facilitate nucleophilic attack upon phosphorus by polarizing the γ-phosphorus−oxygen bond. To test the prediction that the positively charged guanidinium group of R596 in human α_1 Na,K-ATPase participates in phosphoryl group transfer, the charge was progressively decreased by site-directed mutagenesis. Mutants R596K, -Q, -T, -M, -A, -G, and -E were expressed in yeast membranes, and their ability to catalyze phosphorylation with inorganic phosphate was evaluated by following ^{18}O exchange. R596K, in which the positive charge is retained, resembled the wild type. Substitution of a negative charge (R596E) resulted in complete loss of activity. The remaining mutants with uncharged side chains had both lowered affinity for inorganic phosphate and altered phosphate isotopomer distributions, consistent with increased phosphate-off rate constants compared to that of the wild type. Therefore, mutations of R596 strengthen our hypothesis that the oppositely charged side chains of the DPPR peptide in Na,K-ATPase form a quaternary complex with magnesium phosphate.

There is a growing consensus that enzymes evolve by conserving the machinery to catalyze the most difficult step in an overall reaction mechanism (*1*). For example, the initial step in diverse reactions catalyzed by members of the enolase superfamily is abstraction of a proton with an estimated pK_a of >30 from the α-carbon of a carboxylic acid. Acceleration of this step by enolase requires two Mg^{2+} ions (*2*, *3*). Therefore, it was predicted that all members of the enolase superfamily need two Mg^{2+} ions (*4*).

Some mammalian ion pumps are classified as "P-type" because formation of a phosphorylated enzyme intermediate accelerates ATP hydrolysis. The reaction between ATP and a carboxylic acid side chain in the enzyme domain is unlikely because the p*K* for formation of an acyl phosphate from ATP nonenzymatically is 2.2 (*5*). Phosphorylation of the same residue by P_i is even less likely because the p*K* for the nonenzymatic reaction is 7.6 ($\Delta G° \approx 10$ kcal mol^{-1}). Therefore, we proposed a partial model for the active site of P-type ATPases based upon a review of known structures of enzymes that catalyze phosphoryl group transfer (*6*). An explicit assumption was that the dual functionality of pumps evolved by grafting an enzyme onto a channel (*7*).

Our active-site model (*6*) hypothesizes a role for arginine in one (DPPR) of the six signature sequences for P-type pumps (*8*) analogous to the role of lysine in the Walker A (*9*) signature sequence for ATP-binding proteins. The idea of aligning the positive charge on arginine with the positive charge in the phosphate-binding loop (P-loop) formed by the Walker A sequence originated with indirect evidence that aspartic acid in the DPPR sequence of Na,K-ATPase binds Mg^{2+} (*10*). The conclusion that D593 (human α_1 numbering) binds Mg^{2+} was inferred from reduced affinity for negatively charged P_i when the negatively charged carboxylic acid side chain was replaced with an uncharged amide (D593N). This reasoning was checked by testing the prediction that Mg^{2+}

† This research was supported by National Institutes of Health Grant DK52802 (R.A.F. and L.D.F.) and a Veterans Administration Merit Review Award (L.D.F.).

* To whom correspondence should be addressed. Phone: (310) 268-3896. Fax: (310) 268-4963. E-mail: lfaller@ucla.edu.

‡ Department of Physiology and Biophysics, University of Southern California School of Medicine.

§ Department of Biochemistry and Molecular Biology, University of Southern California School of Medicine.

|| CURE: Digestive Diseases Research Center, Department of Medicine, University of California at Los Angeles School of Medicine, and Veterans Administration Greater Los Angeles Health Care System.

⊥ Department of Physiological Sciences, University of California at Los Angeles.

10.1021/bi010270+ CCC: $20.00
Published on Web 05/04/2001

binds before P_i and by searching for examples of ternary enzyme−COO^-·Mg^{2+}·P_i^{2-} complexes in determined structures of enzymes that catalyze phosphoryl group transfer. Experiments with purified pig kidney Na,K-ATPase[1] confirmed that the rate equation for ordered binding fits ^{18}O-exchange data for phosphorylation by P_i better than equations for alternative mechanisms (*7*). Homologous peptides forming quaternary enzyme−COO^-·Mg^{2+}·P_i^{2-}·^+H_3N [or $^+(H_2N)_2$-CNH]−enzyme complexes were found in the crystal structures of a number of phosphoryl group transferases,[2] suggesting that R596 cooperates with D593 in binding MgP_i. Aligning arginine in the DPPR sequence with lysine in the P-loop of enzymes that catalyze phosphoryl group transfer also aligned a predicted helix−coil−strand sequence in P-type pumps with the secondary structural elements of a conserved hairpin. The hairpin juxtaposes the P-loop with other amino acids that are important for catalysis in the crystal structures of AK, AMPSase, DTBS, F_1, and PCK. Therefore, we speculated that this motif might be an additional supersecondary structural signature for Mg^{2+}-dependent phosphoryl group transfer (*6*). The hairpin is present in the recently published crystal structure of SR Ca-ATPase (*12*), where it connects the DPPR sequence to another signature sequence for P-type pumps (MVTGD) containing threonine and aspartic acid residues implicated in function by site-directed mutagenesis (*13*). Aligning R596 with lysine also aligns D593 with aspartic acids in the P-loops of two phosphoryl group transferases (AMPSase and DTBS). The conserved charges form a quaternary complex with MgP_i in at least one of them (AMPSase). D13 in the P-loop of AMPSase is essential for activity and is located 3.16 Å from Mg^{2+} in the crystal structure of the enzyme cocrystallized with the divalent cation and a combination of substrates and products, or their analogues (*14*). A NO_3^- ion between Mg^{2+} (2.56 Å) and K16 (2.73 Å) occupies the presumed position of the phosphoryl group in the transition state during transfer from GTP to IMP in the first step of adenylosuccinate synthesis. Energy minimization calculations indicated that the DPPR peptide of Na,K-ATPase could assume the observed configuration of DEGK coordinated to Mg^{2+} and NO_3^- in the structure of AMPSase (*7*). Therefore, we proposed the DEGK sequence in the P-loop of AMPSase as a model for the DPPR sequence of Na,K-ATPase with arginine functioning like lysine (*6*).

The lysine in P-loops is strictly conserved and has two main functions. First, the positive charge contributes to substrate binding by electrostatic interaction with the polyphosphate moiety, and second, the positive charge participates in catalysis by polarizing the γ-phosphorus−oxygen bond, thereby facilitating nucleophilic attack upon phosphorus. Therefore, if R596 functions like P-loop lysines, both the affinity of Na,K-ATPase for P_i and the catalytic efficiency of the enzyme were expected to progressively decrease when the sign of the charge normally on the side chain was changed from positive to negative. To test these predictions, R596 was replaced with lysine, glutamine, threonine, methionine, alanine, glycine, or glutamic acid, and the ability of the mutant enzymes to bind P_i and catalyze phosphorylation was evaluated by following ^{18}O exchange. Some of the evidence supporting the principal conclusion drawn in this paper, viz., that arginine in the DPPR sequence of Na,K-ATPase binds P_i, has been presented at symposia (*15*, *16*). The results also predict disruption of specific hydrogen bonds observed in the crystal structure of Ca-ATPase (*12*) when the enzyme changes from the E_1 to the E_2 conformation.

EXPERIMENTAL PROCEDURES

Materials

Preparation of Yeast Expression Plasmids. Human Na,K-ATPase α subunit and β subunit cDNAs were obtained from J. Lingrel (University of Cincinnati, Cincinnati, OH). Human α_1 cDNA (3072 base pairs) was released from the pRcCMV plasmid by restriction digestion with *Nco*I and *Dra*III. After the 5′ end had been filled in and exonuclease treatment of the 3′ end, a blunt end fragment was obtained containing 1 base pair of untranslated sequence at the 5′ end and 15 base pairs at the 3′ end. This fragment was then ligated into the *Eco*RI-digested yeast expression plasmid YEp1PT (*17*) to create the expression plasmid YhNα1. Human β_1 cDNA (912 base pairs) was released from the pKC4 vector by digestion with *Bst*XI and *Bcl*I. The 5′ end was cut back, and the 3′ end was filled in by treatment with T4 DNA polymerase, resulting in a blunt-ended fragment without any untranslated base pairs at the 5′ end and with two untranslated base pairs at the 3′ end. The fragment was then ligated into the *Bam*HI-digested and nuclease-treated yeast expression vector pG1T (*18*), in which it is expressed under the control of the inducible GAL1 promoter. The resulting plasmid is designated GhNβ1.

For mutagenesis, a *Bam*HI−*Spe*I fragment was removed from the YhNα1 plasmid and was ligated into *Bam*HI-cut and *Spe*I-cut pKS+ (Stratagene). PCR primers were designed to introduce the desired amino acid change into the Na,K-ATPase α subunit using the QuickChange procedure (Stratagene). The *Bam*HI−*Spe*I fragment was then ligated back into YhNα1, and the presence of the mutation was confirmed by restriction digestion. All mutant cDNAs were sequenced to confirm the presence of the expected mutation and to exclude unexpected mutations.

Expression of Wild-Type and Mutant Human Na,K-ATPase in Yeast. Yeast 30-4 cells (MAT α trp1 ura3 Vn2 GAL+) were transformed with wild-type or mutant YhNα1 plasmids and GhNβ1 plasmids (*19*). Single colonies were selected and were grown as liquid cultures in 0.17% yeast nitrogen base supplemented with ammonium sulfate, adenine, and amino

[1] Abbreviations: Na,K-ATPase, Mg^{2+}-dependent and Na^+- and K^+-stimulated ATPase (EC 3.6.1.37); Ca-ATPase, Ca^{2+}- and Mg^{2+}-dependent ATPase (EC 3.6.1.38); AK, adenylate kinase (EC 2.7.4.3); AMPSase, adenylosuccinate synthetase (EC 6.3.4.4); DTBS, dethiobiotin synthetase (EC 6.3.3.3); F_1, bovine mitochondrial F_1-ATPase (EC 3.6.1.34); H-ATPase, yeast proton ATPase (EC 3.6.1.35); PCK, phosphoenolpyruvate carboxykinase (EC 4.1.1.49); CheY, bacterial chemotaxis regulator; HAD, haloacid dehalogenase; SR, sarcoplasmic reticulum; WT, wild type; XTP, adenosine or guanosine 5′-triphosphate; IMP, inosine 5′-monophosphate; P_i, inorganic phosphate; BSA, bovine serum albumin; ChoCl, choline chloride; DTT, dithiothreitol; EDTA, ethylenediaminetetraacetic acid; HEPES, *N*-(2-hydroxyethyl)piperazine-*N*′-2-ethanesulfonic acid; NADH, reduced nicotinamide adenine dinucleotide; SDS−PAGE, sodium dodecyl sulfate−polyacrylamide gel electrophoresis; TBS(T), Tris saline buffer (Tween 20); Tris, tris(hydroxymethyl)aminomethane; PCR, polymerase chain reaction; AE, average (isotope) enrichment; rms, root-mean-square; SE, standard error; TN, turnover number.

[2] P_i and the protein ligands may be in outer aqueous coordination spheres of the metal ion, e.g., the DGFPR and DMLR peptides of AK (*11*).

acids, except tryptophan and uracil (*20*). Cells were collected, and microsomal membranes were prepared as previously described (*21*). The microsomal membranes were purified with 0.1% (w/v) SDS following a published protocol (*22*).

Synthesis of ^{18}O-Enriched Inorganic Phosphate. Ultrapure PCl_5 (Alpha Products) was reacted with ^{18}O-enriched (>99%) water (Icon) in a drybox to make isotopically enriched P_i (*23*). The measured AE ($\sum_j P^{18}O_j{}^{16}O_{4-j}/4\sum P^{18}O_j{}^{16}O_{4-j}$) of the product ([^{18}O]P_i) was 99.3% with 97.1% containing four ^{18}O atoms. Nonenzymatic oxygen exchange between P_i and water is negligible when solutions are stored at neutral pH.

Methods

Quantitation of Expression Levels by Western Blot Analysis. SDS-extracted yeast membrane protein (10 μg) was loaded onto a 10% SDS−polyacrylamide gel in lanes for each mutant and for the wild-type Na,K-ATPase expressed in yeast. In addition, six different amounts of purified dog kidney Na,K-ATPase (5−100 ng) were loaded onto the same gel to serve as standards. After electrophoresis, the samples were transferred to an Immobilon-P membrane. The membrane was soaked in 0.5% BSA in TBST for at least 1 h at 4 °C, followed by overnight incubation at 4 °C with monoclonal antibody C-464.6 (M. Kashgarian, Yale University, New Haven, CT) which is specific for α_1 subunits. Membranes were washed three times for 10 min each in TBST at 4 °C and were incubated at room temperature for 1 h with rabbit anti-mouse IgG. After incubation with the secondary antibody, the membranes were washed three times at room temperature for 10 min each with TBS. The membranes were incubated with 0.5−1 μCi of [^{125}I]protein A at room temperature for 1 h and then were washed three times at room temperature for 10 min each with TBS. The membranes were rinsed briefly with 80% methanol and were dried in a fume hood. Radiolabeled bands were identified by autoradiography after 0.5−3 day exposures, and pieces of Immobilon-P membrane corresponding to the radiolabeled bands were excised and counted for Cherenkov radiation. The abundance of α subunit relative to the purified dog kidney Na,K-ATPase standards was calculated for each mutant, and the expression level was determined as a percentage of the total SDS-extracted yeast membrane protein, or in picomoles per milligram assuming a molecular mass of 112 kDa for the α subunit.

Quantitation of Expression Levels by [^{3}H]Ouabain Binding. Tritiated-ouabain binding to phosphoenzyme formed from P_i was assessed by the protocol described previously (*10*) with minor variations. SDS-extracted membrane protein (130−470 μg) was incubated with 0.25 nM [^{3}H]ouabain (Du Pont-New England Nuclear, specific activity of 27−30 Ci mmol^{-1}) and increasing concentrations of nonradioactive ouabain (0.25−1000 nM). Maximum ouabain binding capacity (B_{max}) and the ouabain dissociation constant (K_d) were estimated from nonlinear least-squares fits of the equation for binding by a single site to the experimental data. A control experiment in which P_i was replaced with 2 mM Tris-vanadate confirmed that the estimates of B_{max} for mutants were not affected significantly by changes in the P_i dissociation constant. Vanadate is a transition-state analogue of phosphate that binds several orders of magnitude tighter than phosphate to Na,K-ATPase (*24*), virtually ensuring saturation of mutants by millimolar levels of vanadate.

Assay of Na,K-ATPase Activity. Na^+- and K^+-stimulated ATPase activity was measured by enzymatically coupling ATP hydrolysis to NADH oxidation (*25*). As described previously (*10*), reaction mixtures containing the reagents required for the colorimetric assay, 10 mM HEPES-triethylamine buffer adjusted to pH 7.4, 120 mM NaCl, 20 mM KCl, 2.5 mM $MgCl_2$, 1 mM EDTA, 5 mM sodium azide, 1 mM DTT, and from 0.025 to 1 mM ATP, in a final volume of 1 mL were incubated at 37 °C for 15 min. The reaction was started by adding 20−50 μg of SDS-extracted yeast membrane protein, and oxidation of NADH was followed at 340 nm with a Beckman DU-650 spectrophotometer for 30 min at 37 °C. Control measurements in the presence of 0.5 mM ouabain were used to correct for ouabain-insensitive activity. The maximum rate (V_{max}) and Michaelis constant (K_m), which may be an apparent value, were estimated from nonlinear least-squares fits of the Michaelis equation to the experimental data.

Measurement and Analysis of ^{18}O Exchange. The methods used in our laboratory to assess ^{18}O exchange between P_i and water by mass spectrometry and analyze the results have been described in detail previously (*7*). Most of the observed isotope exchange is inhibited by ouabain, when the wild type or mutants are expressed in yeast cells (*10*), because there is no endogenous Na,K-ATPase and the exogenous enzyme binds P_i more than an order of magnitude tighter than the yeast proton ATPase (*26*). Therefore, correction for adventitious P_i introduced with the membranes and ouabain-insensitive exchange was achieved by using the isotopomer distribution estimated for a control experiment in the presence of 0.1 mM ouabain from the ^{18}O-enriched P_i distribution as the starting distribution for Na,K-ATPase-catalyzed (ouabain-inhibitable) exchange. Details of the experiments are given in the figure legends and table footnotes.

Theory of ^{18}O Exchange. We have shown that Na,K-ATPase functions as a metalloenzyme catalyzing ^{18}O exchange between P_i and H_2O by an ordered mechanism in which Mg^{2+} binds before P_i (*7*).

$$E + Mg^{2+} \underset{K_{Mg}}{\rightleftharpoons} MgE + P_i \underset{K_P'}{\rightleftharpoons} MgE{\cdot}P_i \overset{k_{-HOH}}{\underset{k'_{+HOH}}{\rightleftharpoons}} MgE{-}P \quad (1)$$

In eq 1, K_{Mg} is the Mg^{2+} dissociation constant for re-forming the apoenzyme (E); K_P' is the dissociation constant for dissociation of noncovalently bound P_i from the metalloenzyme (MgE); k_{-HOH} is the rate constant for water loss from the Michaelis complex (MgE·P_i) via nucleophilic attack of a carboxyl group on the enzyme upon phosphorus, i.e., phosphorylation of the enzyme; and k'_{+HOH} is a pseudo-first-order rate constant for hydrolysis of the covalent phosphoenzyme (MgE−P) bond that includes the concentration of isotopically unenriched water (55.6 M).

Two parameters can be estimated by fitting equations for the relative amount of each of the five $P^{18}O_j{}^{16}O_{4-j}$ ($0 \le j \le 4$) isotopomers at a single time point (*27*) to the observed isotopomer distribution. The partition coefficient (P_c) is the probability of P_i entering the exchange reaction.

$$P_c = \frac{k_{-HOH}}{k_{-P_i} + k_{-HOH}} \quad (2)$$

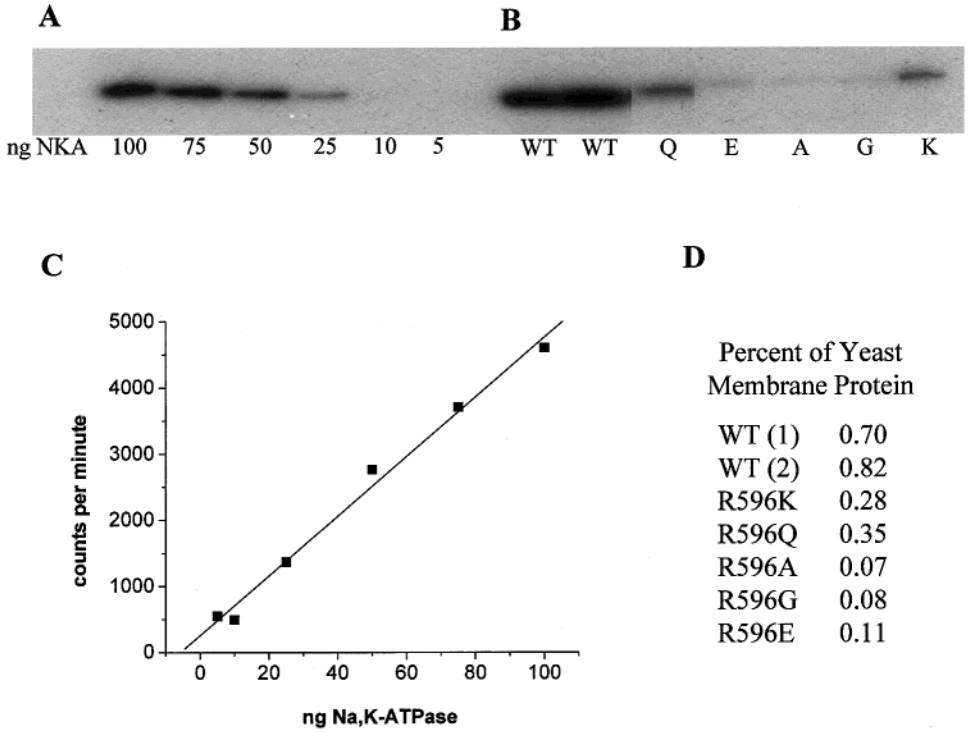

FIGURE 1: Western blot and quantitation of expression levels. (A) Purified dog kidney Na,K-ATPase in the amounts indicated below the blot was separated by SDS−PAGE and immunoblotted as described in Experimental Procedures. The blot shows the autoradiogram obtained after detection exposure of film to the [^{125}I]protein A-labeled samples. (B) Ten micrograms of SDS-extracted yeast membranes containing the wild type (WT) or Na,K-ATPase mutations indicated below the blot were separated and blotted as described for panel A. The blot shows the autoradiogram. (C) Radioactivity is plotted as a function of the amount of Na,K-ATPase shown in each lane of panel A. The line through the data is the least-squares fit of a straight line to the data. (D) The amount of α subunit present in each band of panel B is tabulated as a percentage of the total yeast protein in each sample.

The exchange rate (v_{ex}) is the rate at which unlabeled oxygen enters P_i.

$$v_{ex} = k'_{+HOH}[E{-}P] = V_{max}\frac{[P_i]}{[P_i] + K_{0.5}} \quad (3)$$

For the ordered binding mechanism in eq 1, the maximum rate (V_{max}) is given by eq 4.

$$V_{max} = \frac{k_{+HOH}E_0}{1 + K_{HOH}} \quad (4)$$

E_0 is the total enzyme concentration, and K_{HOH} (k_{-HOH}/k'_{+HOH}) is the equilibrium constant for formation of the phosphorylated enzyme from the Michaelis complex. The half-maximum substrate concentration ($K_{0.5}$) depends inversely upon the Mg^{2+} concentration.

$$K_{0.5} = \frac{K_P'}{1 + K_{HOH}}\left(1 + \frac{K_{Mg}}{[Mg^{2+}]}\right) \quad (5)$$

Therefore, K_{Mg}, $K_P'/(1 + K_{HOH})$, and V_{max} can be estimated from an array of measurements of v_{ex} as a function of total P_i and Mg^{2+} concentrations. The free concentrations of Mg^{2+} and P_i in eqs 3 and 5 were calculated from the total concentrations by assuming a 1:1 complex is formed with a K_d of 8.5 mM (*7*).

RESULTS

Expression Levels of R596 Mutant and Wild-Type Human $\alpha_1\beta_1$ Na,K-ATPase in Yeast. Wild-type human Na,K-ATPase $\alpha_1\beta_1$ and R596 mutants were expressed in *Saccharomyces cerevisiae*, and a microsomal membrane fraction was isolated. After extraction of the membranes with 0.1% (w/v) SDS, the amount of expressed α_1 subunit in each membrane preparation was estimated by Western blotting as described in Experimental Procedures. Expressed α subunits were quantified by Cherenkov counting of the [^{125}I]protein A-labeled samples and by comparing the heterologously expressed subunits to a series of dog kidney Na,K-ATPase standards on the same blot. The results of a representative experiment are shown in Figure 1. The autoradiogram obtained from the samples is shown in the upper part of the figure, and the standard curve is shown below the autoradiogram. In the preparations shown, the level of WT α subunit expression was approximately 0.8% of the yeast membrane protein level after detergent extraction (62−71 pmol mg^{-1}), and the level of mutant α subunit expression ranged between ∼0.1 and 0.5% (6−31 pmol mg^{-1}). Although some of the bands in Figure 1 are difficult to see because of low expression levels, all samples could be accurately quantified by counting ^{125}I. The expression levels for other preparations of the mutants (except R596E) are reported in picomoles per milligram in column 2 of Table 1.

Quantitation of the Functional Pump Number by Ouabain Binding. Na,K-ATPase forms a phosphorylated intermediate from either ATP or P_i, to which ouabain binds with high affinity. Therefore, ouabain binding can be used to identify pumps that are capable of forming the phosphoenzyme from either of these substrates. The K_d and B_{max} values estimated for the P_i-dependent reaction of the WT and mutant protein preparations summarized in Table 1 are reported in columns

Table 1: Summary of Control Assays[a]

	expression[b]		ouabain binding[c]			Na,K-ATPase activity			
	level (pmol mg^{-1})	n	K_d (nM)	B_{max} (pmol mg^{-1})	n	K_m ($\times$10 mM)	V_{max} ($\times 10^2$ μmol min^{-1} mg^{-1})	n	turnover number[d] (s^{-1})
WT	79 $\pm$ 8	2	23 $\pm$ 13	25 $\pm$ 4	3	3.1 $\pm$ 1.0	16.0 $\pm$ 1.4	3	107 $\pm$ 26
R596K	45 $\pm$ 1	2	28 $\pm$ 10	29 $\pm$ 1	3	1.9 $\pm$ 0.3	17.5 $\pm$ 1.0	3	101 $\pm$ 9
R596Q	48 $\pm$ 3	2	45 $\pm$ 7	8.4 $\pm$ 0.7	4	1.4 $\pm$ 0.3	2.5 $\pm$ 0.2	3	50 $\pm$ 8
R596T	20 $\pm$ 1	2	32 $\pm$ 14	1.2 $\pm$ 0.4	4	2.0 $\pm$ 0.8	0.36 $\pm$ 0.02	2	50 $\pm$ 19
R596M	35 $\pm$ 6	2	48 $\pm$ 7	2.9 $\pm$ 0.6	4	1.6 $\pm$ 0.1	0.44 $\pm$ 0.14	3	25 $\pm$ 13
R596A	36 $\pm$ 1	2	35 $\pm$ 19	8.7 $\pm$ 1.2	2	2.0 $\pm$ 0.6	3.4 $\pm$ 0.5	3	65 $\pm$ 19
R596G	24 $\pm$ 2	2	28 $\pm$ 15	1.8 $\pm$ 0.5	3	1.6 $\pm$ 0.7	0.78 $\pm$ 0.06	6	72 $\pm$ 26
R596E	10	1	nd[e]	nd[e]		nd[e]	nd[e]		nd[e]

[a] Parameter estimates are reported $\pm$ standard error. [b] Western blot. [c] Phosphorylation by P_i. [d] V_{max}/B_{max}. The standard error was calculated by propagating the standard errors in the numerator and the denominator. [e] Not determined.

4 and 5, respectively. All of the mutants, with the exception of R596E, could form phosphoenzyme from P_i and could bind ouabain both before detergent extraction and after detergent extraction of the membranes. Ouabain binding levels for R596E were too low to quantify accurately. All ouabain K_d values were within a factor of 2 of the WT value, indicating that the structure of the ouabain binding site is not likely to be affected by the mutations. Expression levels of α subunits were higher in every case than the number of functional pumps determined by ouabain binding. There are at least two possible reasons for this difference. First, the difference may be related to the use of two different plasmids to express the α and β subunits of Na,K-ATPase. After transformation of yeast, the plasmids are likely to be present in the cells in different copy numbers, and since both α and β subunits must assemble together to form functional pumps (*28*), functional expression is limited by the less abundant subunit. In these mutants, the β subunit appears to be the limiting factor. A similar observation has been made with other mutants and chimeras expressed in yeast, where the limiting abundance of the β subunit protein has been confirmed by Western blotting with anti-β antibodies (*29*). Second, the proteins expressed in yeast may be more easily denatured by SDS extraction than Na,K-ATPase in mammalian membranes. The antibody used to measure α subunit abundance recognizes both functional and nonfunctional polypeptides.

Effects of Mutations to R596 on Na,K-ATPase Activity. With the exception of R596E, all of the mutants were able to catalyze ouabain-sensitive ATP hydrolysis (Table 1). The estimated K_m values of the mutants that do catalyze ATP hydrolysis are not statistically different from the WT value (column 7). The turnover number (TN) in column 10 was calculated by dividing the maximum ATPase activity (V_{max}) by the ouabain binding capacity (B_{max}) for each sample, to compare the activities of the mutants with that of wild-type Na,K-ATPase expressed at different levels. The percentage SE in the quotient is the sum of the percentage standard errors in the numerator and the denominator. As expected for the hypothesized role of arginine in phosphoryl group transfer, the R596K mutant, which retains a positive charge on the amino acid side chain, had normal Na,K-ATPase activity. Loss of the positive charge was associated with a reduction in activity in all of the mutants with uncharged amino acid side chains, and replacement of the positive charge with a negative charge in the R596E mutation resulted in an inactive enzyme. However, it was not possible to rank the effects of the uncharged amino acid substitutions on activity because the aggregate uncertainty in the estimates of V_{max} and B_{max} was too great.

Table 2: Comparison of Observed with Fitted Isotopomer Distributions for R596K[a]

isotopomer	observed (%)	fitted[b] (%)	residual (%)
$P^{18}O_4$	33.80	34.08	−0.27
$P^{18}O_3{}^{16}O_1$	35.14	34.93	0.20
$P^{18}O_2{}^{16}O_2$	20.40	21.23	−0.84
$P^{18}O_1{}^{16}O_3$	8.25	8.01	0.24
$P^{16}O_4$	2.42	1.75	0.67

[a] $[Mg^{2+}]_{free}$ = 1 mM. $[P_i]_{free}$ = 5 mM. t = 2 h. AE = 72.4%. [b] P_c = 0.20, and v_{ex} = 0.076 μatom min^{-1} mg^{-1}.

Effects of Mutations to R596 on ^{18}O Exchange. The exchange parameters v_{ex} and P_c can be estimated from the isotopomer distribution at a single time (t) point. Table 2 shows a typical example for one pair of free Mg^{2+} and P_i concentrations in a mutant R596K array. Fewer than 6 pmol of expressed R596K was required to measure the isotopomer distribution in the presence and absence of ouabain. The fitted distribution in column 3, assuming the observed distribution plus ouabain as the starting distribution, is compared with the observed distribution in the absence of ouabain (column 2). The fit is slightly poorer if the isotopomer distribution of the synthesized $[^{18}O]P_i$, which does not take into account adventitious $P^{16}O_4$, is used as the starting distribution (correlation coefficient of 0.99898, compared with 0.99926 for the fit in column 3), but the fitted isotopomer distribution is not significantly different [$P^{18}O_4$ (34.12%), $P^{18}O_3{}^{16}O_1$ (34.93%), $P^{18}O_2{}^{16}O_2$ (21.34%), $P^{18}O_1{}^{16}O_3$ (8.08%), and $P^{16}O_4$ (1.53%)] because only 4% of the exchange was catalyzed by ouabain-insensitive enzymes in the yeast membranes. The square root of the sum of the residuals in column 4 squared is 1.2%, and the rms residual is 0.5%. In Figure 2, the observed distribution in Table 2 for R596K (AE = 72.4%) is compared with a point in an R596A array with approximately the same AE (75.9%). Visible skewing of the R596K distribution (solid bars) compared to the R596A distribution (open bars) toward P_i molecules containing fewer ^{18}O atoms shows that the small difference (0.17) between a P_c of 0.20 (R596K) and a P_c of 0.030 (R596A) can be measured easily. For example, the observed difference between the $P^{18}O_3{}^{16}O_1$ peaks was 5.42%, whereas the sum of the rms residuals in the estimates of the isotopomer percentages for the two mutants was only 0.55%.

Figure 3 shows that $K_{0.5}$ depended inversely upon the free Mg^{2+} concentration as predicted by eq 5. Two arrays of v_{ex} measurements as a function of free Mg^{2+} and P_i concentra-

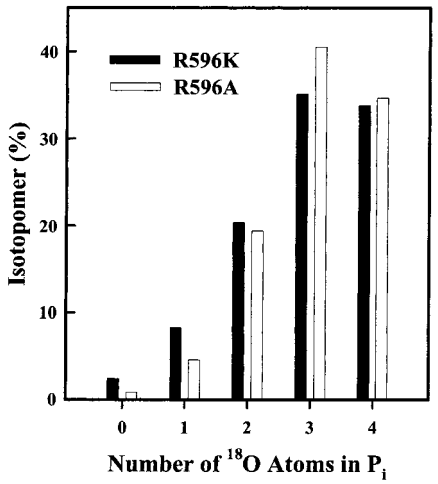

FIGURE 2: Effect of P_c on isotopomer distribution. Observed isotopomer distributions after catalyzing approximately the same amount of exchange with different P_c values are compared. The P_c values estimated from the distributions, with the distribution of a control experiment in which ouabain was present (not shown) as the starting distribution, were 0.20 for R596K (AE = 72.4%) and 0.030 for R596A (AE = 75.9%). Details of the experiment are given in Table 2 for mutant R596K. For R596A, t was 4 h with the following parameters: $[Mg^{2+}]_{free}$ = 2 mM, $[P_i]_{free}$ = 4 mM, and estimated v_{ex} = 0.037 μatom min^{-1} mg^{-1}.

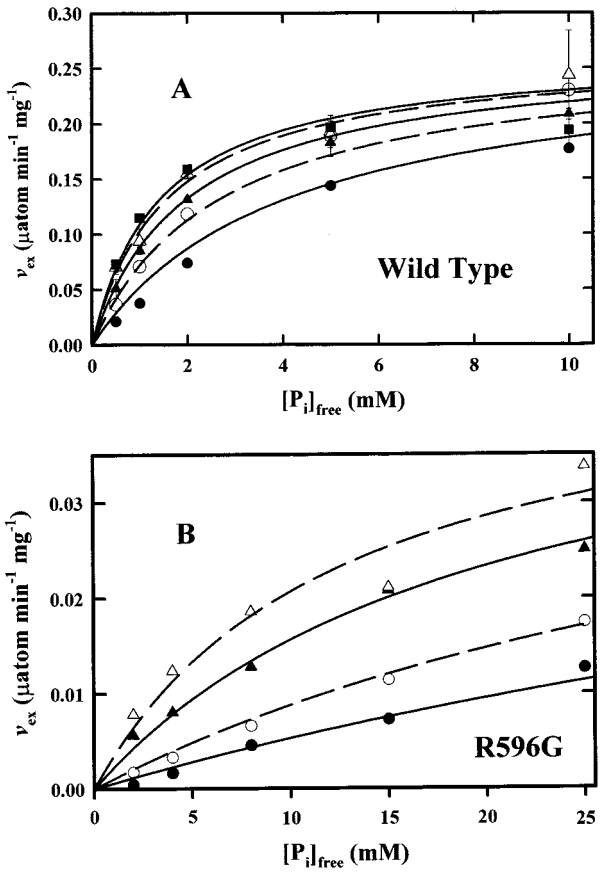

FIGURE 3: Dependence of the ^{18}O-exchange rate on Mg^{2+} and P_i concentrations. The isotope exchange rate (v_{ex}) is plotted vs free P_i concentration for different fixed concentrations of free Mg^{2+}. All measurements were taken at 30 °C and pH 7.4 in 100 mM Tris-HCl buffer containing 10 mM KCl, 0.25 mM sodium azide, the free concentration of P_i shown on the abscissa, enough ChoCl to adjust the ionic strength to 150 mM, and different fixed concentrations of free Mg^{2+}. The total volume was 200 μL. (A) WT (0.37 mg/mL) after 3 h with 0.5 (●), 1 (○), 2 (▲), 5 (△), or 10 mM free Mg^{2+} (■). Points from two separate arrays are shown with points at 1, 2, and 5 mM free Mg^{2+} averaged and the scatter indicated by error bars, when it was greater than the size of the symbol. (B) R596G (0.74 mg/mL) after 4 h with 0.125 (●), 0.25 (○), 0.75 (▲), or 2 mM free Mg^{2+} (△).

tions were combined without any normalization to show the reproducibility of data for the same expressed WT preparation (Figure 3A) and are compared with an array for R596G with uncharged side chain (Figure 3B). The range of half-maximum free P_i concentrations is visibly higher for the mutant than for WT because only the observed WT exchange rate approached saturation despite the broader range of P_i concentrations used to study the mutant. The parameter estimates (±standard error) obtained from global fits of the rate equation (eq 3) to data for all the Mg^{2+} concentrations in each array simultaneously were as follows: $K_{Mg} = 1.1 \pm 0.2$ mM, $K'_P/(1 + K_{HOH}) = 1.3 \pm 0.2$ mM, and $V_{max} = 0.26 \pm 0.01$ μatoms min^{-1} mg^{-1} for WT (n = 40) and $K_{Mg} = 1.1 \pm 0.3$ mM, $K'_P/(1 + K_{HOH}) = 8.0 \pm 2.1$ mM, and $V_{max} = 0.046 \pm 0.004$ μatoms min^{-1} mg^{-1} for R596G (n = 20). In contrast to $K'_P/(1 + K_{HOH})$, which was significantly larger (6-fold) for the mutant than for WT, K_{Mg} was the same within experimental error. The estimates of V_{max} were also significantly different for the plotted arrays. However, V_{max} values cannot be compared directly because the exchange rate is expressed per milligram of total membrane protein. The fraction of the observed exchange that can be inhibited by ouabain ranged from 89 to 97% for WT and from ~40 to 90% for R596G.

The bar graph in Figure 4 shows the effect of changing the sign of the charge on the side chain of amino acid 596. In contrast to Figure 2, which compares observed isotopomer distributions for two different mutants, observed distributions for the same mutant in the presence (solid bars) or absence (open bars) of ouabain (n = 1) are plotted in Figure 4. No inhibition by ouabain was detectable after incubation for 3 h with R596E, in which the side chain is negatively charged. The observed reduction in AE from 99.3 to 84.9% because of ouabain-insensitive exchange was greater than in the ouabain control (not shown) for R596G (Figure 3B) at comparable free Mg^{2+} and P_i concentrations (95.9%) because nearly 7 times more membrane protein was used in an effort to detect exchange catalyzed by R596E.

The exchange parameters estimated from all of the arrays for WT and mutants are summarized in Table 3. Ouabain-inhibitable exchange by R596T could be detected but was not fast enough for determination of an array. The reason is that exchange catalyzed by the expressed human enzyme became nonlinear with time after ~4 h, in contrast to expressed sheep enzyme, which was stable for up to 20 h (*10*). Results for the other mutants fall into three categories. In the first category, the positive charge on the side chain was retained. The exchange properties of R596K were experimentally indistinguishable from those of WT. In the second category, the positive charge was replaced with a negative charge. No exchange catalyzed by R596E could be detected (Figure 4). The remaining mutants are in the third category with uncharged side chains. In every case, neutralization of the positive charge normally on amino acid 596 resulted in (a) unchanged affinity for Mg^{2+} (column 3) compared to that of WT, (b) reduced affinity for P_i and/or a

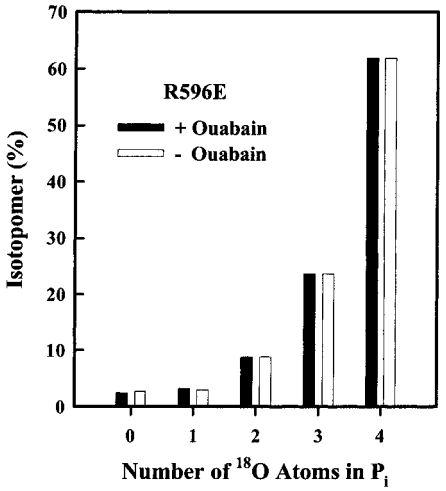

FIGURE 4: Mutant R596E did not catalyze ^{18}O exchange. The isotopomer distributions observed after reacting [^{18}O]P_i with membranes containing R596E for 3 h at 30 °C in the presence (solid bars) and in the absence (open bars) of 0.1 mM ouabain are compared. The free Mg^{2+} concentration was 2 mM; the free P_i concentration was 5 mM, and the protein concentration was 2.4 mg/mL. Other conditions are given in the legend of Figure 3.

Table 3: Summary of ^{18}O-Exchange Parameter Estimates[a]

	N[b]	K_{Mg} (mM)	$K'_P/(1+K_{HOH})$ (mM)	P_c	V_{max} ($\times 10^2$ μatom min^{-1} mg^{-1})
WT	4	0.9 ± 0.1	2.0 ± 1.0	0.22 ± 0.04	30 ± 2
R596K	2	0.7 ± 0.2	2.0 ± 0.2	0.22 ± 0.04	36 ± 24
R596Q	2	0.8 ± 0.1	14 ± 2	0.04 ± 0.01	10 ± 2
R596T	0	nd[c]	nd[c]	nd[c]	nd[c]
R596M	1	1.1 ± 0.2	9 ± 1	0.02 ± 0.01	6.3 ± 0.3
R596A	3	0.7 ± 0.1	14 ± 6	0.04 ± 0.01	17 ± 5
R596G	3	1.3 ± 0.3	11 ± 5	0.03 ± 0.02	5 ± 1
R596E	0	nd[c]	nd[c]	nd[c]	nd[c]

[a] Mean ± SE. [b] Number of arrays of n (14−34) measurements of $v_{ex} = f([Mg^{2+}]_{free},[P_i]_{free})$. [c] Not determined.

shift in the MgE·P_i ⇌ MgE−P equilibrium toward MgE·P_i (column 4), and (c) lowered P_c values (column 5). The differences between the parameter estimates for the uncharged mutants are not statistically significant. Therefore, the mean values (±standard error) were calculated giving the following exchange parameter estimates for uncharged mutants: $K_{Mg} = 1.0 \pm 0.1$ mM, $K'_P/(1 + K_{HOH}) = 12.4 \pm 2.4$ mM, and $P_c = 0.035 \pm 0.004$ ($N = 9$). Although uncharged mutants generally had lower measured exchange rates than WT, the expression levels (Figure 1 and Table 1, column 2) were also lower and the fraction of protein detected by Western blot that bound ouabain was much lower (cf. columns 2 and 5 of Table 1). Turnover numbers are not tabulated because the scatter in values calculated with V_{max} and B_{max} estimates for different mutant preparations (SE = 25−53%) precluded meaningful comparison with those of WT. However, the TN estimated for WT (215 ± 16 s^{-1}, $N = 4$) is in reasonable agreement with the value (250 s^{-1}) obtained from studies of purified pig kidney enzyme (*7*, *10*).

DISCUSSION

In determined structures of P-loop-containing enzymes that catalyze nucleotide triphosphate hydrolysis, the positively charged side chain of lysine is positioned to bind negatively charged P_i and polarize the γ-phosphorus−oxygen bond, facilitating nucleophilic attack by an acceptor. Transfer of the phosphoryl group occurs via a pentacoordinate intermediate (*30*) with inversion of the chirality of phosphorus (*31*). There is evidence that P-type ATPases catalyze phosphoryl group transfer by the same mechanism. The acceptor is a carboxyl group on the protein (*32*); pentacoordinate orthovanadate is a transition-state analogue (*24*); and phosphorylation and dephosphorylation of the enzyme (two transfers of the same phosphoryl group) occur with retention of configuration (*33*). If R596 of human Na,K-ATPase is functionally equivalent to the lysine of P-loop-containing phosphoryl group transferases, the simplest predictions based upon charge type for the ^{18}O-exchange activity of the mutants made to test the theory are as follows. First, R596K should resemble WT because the positive charge is retained. Second, R596E might not bind P_i and be inactive because the negative charge repulses P_i. Third, R596Q, R596T, R596M, R596A, and R596G should have reduced affinity for P_i and activities paralleling the polarizability of their uncharged side chains.

Evidence for Correct Folding. Figure 1 and Table 1 show that all of the mutants were expressed in yeast cells and that all of them bound ouabain and catalyzed ATP hydrolysis except R596E. The affinity of WT for ouabain is indistinguishable from the affinity of Na,K-ATPase in human tissue homogenates (unpublished experiments) for ouabain (K_d = 18 ± 6 nM). The TN estimated for WT (∼100 s^{-1}) falls between values of TN estimated from V_{max} and B_{max} measurements for Na,K-ATPase purified from other sources, such as shark rectal (70 s^{-1}) gland (*34*) and duck nasal (160 s^{-1}) glands (*35*). It is almost identical to the TN (111 s^{-1}) recently obtained for sheep $\alpha_1\beta_1$ Na,K-ATPase expressed in insect cells (*36*). Therefore, WT human Na,K-ATPase expressed in yeast cells appears to function normally. The estimated ouabain affinities and Michaelis constants also indicate correct folding of all the mutants except R596E. The ouabain affinities (column 4) of R596K, -Q, -T, -M, -A, and -G are indistinguishable from that of WT (row 1), and the Michaelis constants (column 7) are indistinguishable from the value obtained in this study for WT (row 1), or in other studies from this laboratory (unpublished experiments) for WT human $\alpha_1\beta_1$ expressed in yeast (208 μM). The mean turnover numbers estimated for all of the mutants with uncharged side chains are lower than the mean value for WT, but the mutants are not statistically distinguishable from each other (column 10). The reduction in TN of mutants to 23−67% of the WT value falls within the range reported previously for the ATPase and transport activities of mutants in which the corresponding arginine of yeast plasma membrane H-ATPase (*37*) or SR Ca-ATPase (*13*) was changed. Reductions in H-ATPase activity to between 10 and 60% of that of WT were provisionally attributed to a reduced affinity for ATP; however, the estimated K_m values were within a factor of 2 of that of WT, and the uncertainties in the estimates were not reported (*37*). A lower affinity for ATP was ruled out as the cause of the reduced transport activity by the mutation R604M in Ca-ATPase because the percentage of WT transport activity was approximately the same with ATP (65%) or acetyl phosphate (70%) as the energy source (*13*). Changes in activities dependent upon multiple steps in the catalysis-transport cycle are inherently difficult

to interpret unambiguously because the reactions are chemically coupled.

Evidence That R596 Binds P_i. In contrast to Na^+- and K^+-dependent ATP hydrolysis, catalysis of ^{18}O exchange between P_i and water in the presence of a saturating concentration of K^+ involves only two discrete steps in the overall reaction cycle, viz., P_i binding and phosphorylation and dephophorylation of the enzyme (eq 1). The exchange parameters summarized in Table 3 confirm the first two predictions made by equating R596 with lysine in the P-loops of other enzymes that catalyze Mg^{2+}-dependent ATP hydrolysis. In agreement with the first prediction, R596K, in which the positive charge on the side chain was retained, resembled WT in all of its ^{18}O-exchange properties. R596E, in which the sign of the charge was changed from positive to negative, was inactive, consistent with the second prediction, although incorrect folding of the negatively charged mutant cannot be ruled out. The third prediction is partially confirmed. The estimates of $K'_P/(1 + K_{HOH})$ were higher for all of the mutants with uncharged side chains than for WT (column 4). The observed increase in $K'_P/(1 + K_{HOH})$ could result from an increase in K'_P, a decrease in K_{HOH}, or some combination of the two. It is unlikely that the average observed increase (~6-fold) in $K'_P/(1 + K_{HOH})$ could result entirely from a shift in the equilibrium between $MgE{\cdot}P_i$ and $MgE-P$ toward $MgE{\cdot}P_i$ for the following reason. Estimates of K_{HOH} from the effect of K^+ on the stoichiometry of metalloenzyme phosphorylation ranging from 0.5 (*38*) to 1 (*39*) bracket our estimate (0.59) from ^{18}O-exchange measurements with Na,K-ATPase purified from pig kidneys (*7*). Therefore, a decrease in K_{HOH} could only account for a 2-fold increase in $K'_P/(1 + K_{HOH})$. On the other hand, both the observed increase in $K'_P/(1 + K_{HOH})$ and the roughly comparable 6-fold decrease in P_c (column 5) caused by neutralizing the charge on R596 can be consistently explained by an increase in K'_P resulting from an increase in the P_i-off rate. An ~7.5-fold increase in k_{-P_i} would be needed to explain the lower P_c of the uncharged mutants compared to that of WT, if k_{-HOH} is not affected. The theoretical value of $K'_P/(1 + K_{HOH})$, calculated by increasing k_{-P_i} 7.5-fold and assuming k'_{+HOH} is also unaffected (15 mM), is only about one standard error from the mean value (12.4 ± 2.4 mM) calculated by averaging the estimates from all of the arrays ($N = 9$) for uncharged mutants (Results). Therefore, the simplest explanation of the ^{18}O-exchange results is that neutralization of the side chain charge in position 596 increases the P_i-off rate. The corollary expectation that participation of the positive charge on R596 in P_i binding would increase the phosphorylation rate by polarizing the phosphorus−oxygen bond could not be confirmed by the ^{18}O-exchange results. Within experimental error, the mean turnover numbers for ^{18}O exchange catalyzed by mutants were not different from the TN for exchange catalyzed by WT. However, an additional prediction based upon ^{18}O-exchange studies of purified Na,K-ATPase was also confirmed. Since Mg^{2+} binds before P_i (*7*), no change in K_{Mg} was predicted,[3] and none was observed. K_{Mg} was unaffected by the mutations within experimental error (column 3). The estimates of K_{Mg} and $K'_P/(1 + K_{HOH})$ for the WT human enzyme expressed in yeast cells differ somewhat from the values (3.8 ± 0.6 and 0.57 ± 0.07 mM, respectively) obtained for the enzyme purified from pig kidneys (*7*), but P_c was the same within experimental error (0.26 ± 0.03). Moreover, the Michaelis constant estimated by fitting the Michaelis equation to the 2 mM Mg^{2+} data in Figure 3A (1.9 ± 0.1 mM) is not significantly different from the K_m obtained for sheep kidney enzyme expressed in yeast membranes (1.5 ± 0.2 mM), and P_c (0.20 ± 0.02) was the same (*10*). The small differences in affinity for Mg^{2+} and P_i of WT expressed in yeast membranes compared to the affinities of the enzyme isolated from natural membranes (both purified by SDS extraction) could result from species differences, or from the different lipid environments of the protein in natural and yeast membranes.

Interpretation of the Results. The evidence from internal comparison of mutants with WT of the same species expressed in yeast membranes for increased $K'_P/(1 + K_{HOH})$ (Figure 3) and reduced P_c (Figure 2) is compelling. The fact that both changes can be explained by a 7.5-fold increase in the P_i-off rate does not mean that other rate constants for the partial reactions involved in ^{18}O exchange (eq 1) are unaffected. However, the dominant effect appears to be on k_{-P_i}, resulting in a reduced affinity for P_i, if published estimates of K_{HOH} (*7*, *38*, *39*) are correct. The effects of neutralizing the charge on D593 on $K'_P/(1 + K_{HOH})$ and P_c could also be explained by an increase in the P_i-off rate (*10*). The other effect of neutralizing the charge on R596 appears to be slower turnover of the complete reaction cycle (Table 1). The D593N mutation (*10*) lowered the TN for ATP hydrolysis to about the same percentage (32%) of WT as mutations of R596 (23−67%). The explanation could be either a direct effect on the step limiting the rate of ATP hydrolysis by WT or a change in rate-limiting step caused by the mutations. The reactions in eq 1 are not normally rate-limiting. Expressed WT Na,K-ATPase catalyzed ^{18}O exchange (TN ≈ 200 s^{-1}) twice as fast as ATP hydrolysis (TN ≈ 100 s^{-1}), and increasing the P_i-off rate would not be expected to slow the reaction cycle. A more likely candidate for a step that might become rate-limiting is the $E_1-P \rightarrow E_2-P$ conformational change. MacLennan (*13*) concluded that neutralizing the charge on the aspartic acid in Ca-ATPase corresponding to D593 (D601N) slowed the $E_1-P \rightarrow E_2-P$ transition without affecting dephosphorylation of the E_2 conformation. Neutralizing D593 or R596 might also slow the $E_2{\cdot}ATP \rightarrow E_1{\cdot}ATP$ transition, which is generally considered to be rate-limiting for the sodium pump reaction cycle (*41*, *42*). Therefore, the DPPR sequence may be important for conformational stabilization of the pump as well as phosphoryl group transfer.

Implications for the Structure of the E_2 Conformation of Na,K-ATPase. While the research reported in this paper was in progress, the first high-resolution structure of a P-type ATPase was published (*12*). Figure 5 shows the structure of the hairpin connecting the DPPR (residues 601−604) sequence to a threonine (T625) and an aspartic acid (D627) implicated in function by site-directed mutagenesis (*13*) and the spatial arrangement of the DPPR sequence in the open (presumably E_1) conformation of SR Ca-ATPase with two Ca^{2+} ions bound (*12*). The phosphoryl group acceptor (D351)

[3] A tacit assumption is that Mg^{2+} is effectively screened, e.g., by water, from charge on the side chain of amino acid 596 in the apoenzyme. A precedent for this assumption is statistical binding of two Mn^{2+} ions to sites separated by 4.2 Å in the crystal structure of yeast inorganic pyrophosphatase (*40*).

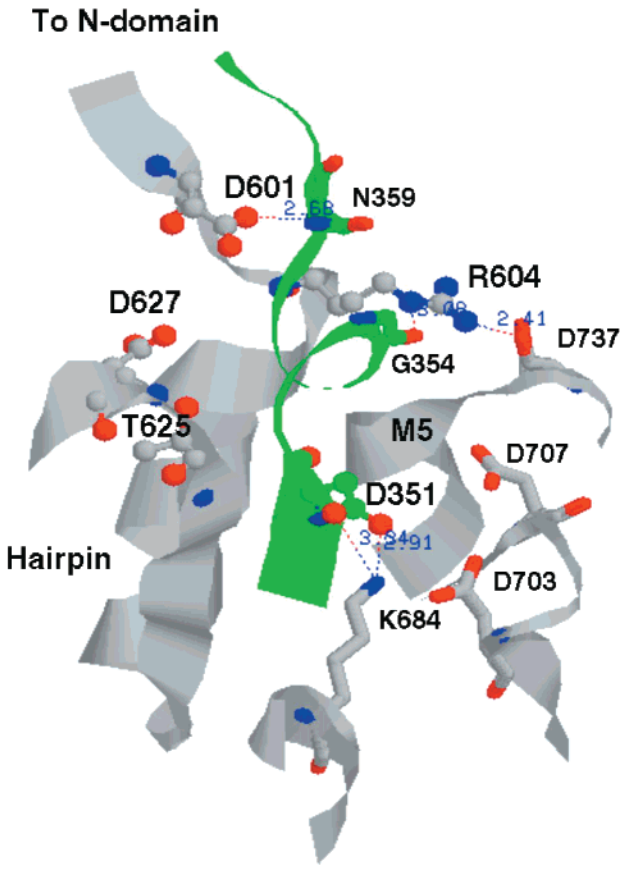

FIGURE 5: Hinge region of Ca-ATPase. The putative phosphorylation site in the open conformation of Ca-ATPase is shown (*12*). The coil (green) after D351 (Ca-ATPase numbering) in the signature DKTGT sequence connects the phosphorylation domain to the nucleotide-binding domain. The coil containing D601 and R604 reconnects the N-domain to the P-domain. The hairpin (β-strand in front with α-helix behind) connecting signature sequences (DPPR and MVTGD) in our model for the active site (*6*) is on the left. Hydrogen bonds between D601 and N359 (2.68 Å) and between D604 and both G354 (3.08 Å) and D737 (2.41 Å) stabilize the open conformation. D351 points toward K684 because of hydrogen bonds (2.91 and 3.34 Å) to K684. T625 and K684 participate in phosphoryl group transfer in the HAD model (*48*), and D703 and D707 in the signature TGDGVND sequence bind Mg^{2+} (*44*).

and the DPPR sequence are located in two coils forming the only tenuous connections between the nucleotide-binding (N) and phosphorylation (P) domains of the protein. The nucleotide binding (not shown) and phosphorylation sites are separated by more than 25 Å, in good agreement with the distance estimated for their separation in the E_1 conformation of Na,K-ATPase ($\leq$29 Å) by energy transfer measurements (*43*). The carboxyl group of D351 points away from the putative MgP_i binding site in our model toward two carboxyl groups (D703 and D707), which have been proposed as ligands for the metal (*44*), because of interactions with a lysine side chain (K684). Similarly, the side chain of arginine (R604) points away from the carboxyl group (D601) that coordinates MgP_i in our model because of hydrogen bonds to backbone carbonyls in coils connecting the P-domain to the N-domain (G354) and to the transmembrane (M) domain (D737). Toyoshima et al. (*12*) proposed that the network of hydrogen bonds between the positively charged side chain of R604 and amino acids in other coils connecting the N-, P-, and M-domains links the large relative movement of the N- and P-domains required for catalysis to the Ca^{2+} binding sites in the M-domain. D601 is also hydrogen bonded to the backbone nitrogen of N359 in the coil (green) after D351 connecting the P-domain to the N-domain. Therefore, another consequence of disrupting the hinge region by neutralizing the charge on either D601 or R604 could be slower transitions between the E_1 and E_2 conformations, as proposed by MacLennan (*13*).

The ^{18}O-exchange experiments described in this report were not designed to detect domain movements. Conversely, it is extremely unlikely that the evidence summarized in Table 3 for reduced P_i affinities and altered isotopomer distributions of uncharged mutants can be explained by a protein conformational change. The ^{18}O-exchange rate in mixtures of Na^+ and K^+ is proportional to the fraction of the enzyme in the E_2 conformation with Mg^{2+} and two K^+ ions bound, calculated with equations derived for a concerted change in the conformation of the unphosphorylated enzyme (*45*) and monovalent cation dissociation constants (*46*) from the metalloenzyme (unpublished experiments). Ten times the Mg^{2+} and K^+ concentrations needed to shift Na,K-ATPase entirely into the E_2 conformation were used to avoid any ambiguity in the interpretation of ^{18}O-exchange data because of coupling between the reactions in eq 1 and the $E_1 \rightleftharpoons E_2$ equilibrium. The substrate is P_i, which presumably must occupy the γ-phosphate site in the exchange reaction. Therefore, confirmation of nearly all the predictions of our active-site model is strong evidence that the oppositely charged side chains of DPPR bind MgP_i near the carboxyl acceptor in the E_2 conformation of P-type ATPases. We propose that the hydrogen bonds constraining D601, R604, and D351 in the open conformation of Ca-ATPase (Figure 5) are broken so that the side chains are free to rotate in the closed conformation and the coil (green) connecting the P- and N-domains is disrupted. There is evidence from iron-catalyzed oxidative cleavage that the MVTGD sequence containing T625 and D627 is closer to the signature DKTGT sequence containing D351 in the E_2 conformation of Na,K-ATPase than in the E_1 conformation (*47*).

Roles for T625, K684, and D707 (Figure 5) in phosphoryl group transfer are predicted by the HAD model (*48*) based upon the similarity between the folds of the P-domain and members of the HAD superfamily, such as L-2 haloacid dehalogenase and phosphoserine phosphatase. D627 and the DPPR sequence are not in the HAD model. Roles for D703 and D707 in the signature TGDGVND sequence in Mg^{2+} binding were inferred from alignment of HAD superfamily members with members of the CheY superfamily (*44*) and are supported by site-directed mutagenesis of the aspartic acid corresponding to D703 in Na,K-ATPase (*49*) and by studies of Mg^{2+} binding to a 38-amino acid peptide containing D703 and D707 (*50*). However, a more recent study of mutations in Na,K-ATPase concludes that amino acids in the TGDGVND sequence corresponding to D703 and N706 in Ca-ATPase are not responsible for high-affinity Mg^{2+} binding in the E_2 conformation (*51*), consistent with our hypothesis for the E_2 phosphorylation site. In the HAD model, K684 coordinates P_i polarizing the γ-phosphorus−oxygen bond instead of R604. K684R could be phosphorylated by ATP, but not by P_i (*52*). The structure of a P-type pump crystallized with Mg^{2+} and P_i, or a transition-state analogue like vanadate bound, is needed to decide whether

both positively charged amino acids (R604 and K684) in addition to Mg^{2+} are required to overcome the energy barrier to formation of a carboxylic−phosphoric anhydride from P_i ($\Delta G^\circ \approx 10$ kcal mol^{-1}).

REFERENCES

1. Petsko, G. A., Kenyon, G. L., Gerlt, J. A., Ringe, D., and Kozarich, J. W. (1993) *Trends Biochem. Sci. 18*, 372−376.
2. Faller, L. D., Baroudy, B. M., Johnson, A. M., and Ewall, R. X. (1977) *Biochemistry 16*, 3864−3869.
3. Larsen, T. M., Wedekind, J. E., Rayment, I., and Reed, G. H. (1996) *Biochemistry 35*, 4349−4358.
4. Babbitt, P. C., Hasson, M. S., Wedekind, J. E., Palmer, D. R. J., Barrett, W. C., Reed, G. H., Rayment, I., Ringe, D., Kenyon, G. L., and Gerlt, J. A. (1996) *Biochemistry 35*, 16489−16501.
5. Pickart, C. M., and Jencks, W. P. (1984) *J. Biol. Chem. 259*, 1629−1643.
6. Smirnova, I. N., Kasho, V. N., and Faller, L. D. (1998) *FEBS Lett. 431*, 309−314.
7. Kasho, V. N., Stengelin, M., Smirnova, I. N., and Faller, L. D. (1997) *Biochemistry 36*, 8045−8052.
8. Serrano, R. (1989) *Annu. Rev. Plant Physiol. Plant Mol. Biol. 40*, 61−94.
9. Walker, J. D., Saraste, M., Runswick, M. J., and Gay, N. J. (1982) *EMBO J. 1*, 945−951.
10. Farley, R. A., Heart, E., Kabalin, M., Putnam, D., Wang, K., Kasho, V. N., and Faller, L. D. (1997) *Biochemistry 36*, 941−951.
11. Abele, U., and Schulz, G. E. (1995) *Protein Sci. 4*, 1262−1271.
12. Toyoshima, C., Nakasako, M., Nomura, H., and Ogawa, H. (2000) *Nature 405*, 647−655.
13. Clarke, D. M., Loo, T. W., and MacLennan, D. H. (1990) *J. Biol. Chem. 265*, 22223−22227.
14. Poland, B. W., Fromm, H. J., and Honzatko, R. B. (1996) *J. Mol. Biol. 264*, 1013−1027.
15. Farley, R. A., Elquza, E., Kane, D. J., Kasho, V., and Faller L. D. (2000) *Biophys. J. 78*, 279A.
16. Faller, L. D., Kasho, V. N., Kane, D. J., Elquza, E., and Farley, R. A. (2000) *J. Gen. Physiol. 116*, 17a−18a.
17. Hitzeman, R. A., Leung, D. W., Perry, L. J., Kohr, P. W., Levine, H. L., and Goeddel, D. V. (1983) *Science 219*, 620−625.
18. Eakle, K. A., Horowitz, B., Kim, K. S., Levenson, R., and Farley, R. A. (1991) in *The Sodium Pump: Recent Developments* (Kaplan, J. H., and De Weer, P., Eds.) pp 125−130, Rockefeller University Press, New York.
19. Elble, R. A. (1992) *BioTechniques 13*, 18−20.
20. Sherman, F., Fink, G. R., and Hicks, J. B. (1986) in *Laboratory Course Manual for Methods in Yeast Genetics*, p 165, Cold Spring Harbor Laboratory Press, Plainview, NY.
21. Eakle, K. A., Kim, K. S., Kabalin, M. A., and Farley, R. A. (1992) *Proc. Natl. Acad. Sci. U.S.A. 89*, 2834−2838.
22. Eakle, K. A., Kabalin, M. A., Wang, S.-G., and Farley, R. A. (1994) *J. Biol. Chem. 269*, 6550−6557.
23. Stempel, K. E., and Boyer, P. D. (1986) *Methods Enzymol. 126*, 618−639.
24. Cantley, L. C., Jr., Cantley, L. G., and Josephson, L. (1978) *J. Biol. Chem. 253*, 7361−7368.
25. Barnett, R. E. (1970) *Biochemistry 9*, 4644−4648.
26. Amory, A., Goffeau, A., McIntosh, D. B., and Boyer, P. D. (1982) *J. Biol. Chem. 257*, 12509−12516.
27. Hackney, D. D. (1980) *J. Biol. Chem. 255*, 5320−5328.
28. Horowitz, B., Eakle, K. A., Scheiner-Bobis, G., Randolph, G. R., Chen, C. Y., Hitzeman, R. A., and Farley, R. A. (1990) *J. Biol. Chem. 265*, 4189−4192.
29. Farley, R. A., Schreiber, S., Wang, S.-G., and Scheiner-Bobis, G. (2001) *J. Biol. Chem. 276*, 2608−2615.
30. Knowles, J. R. (1980) *Annu. Rev. Biochem. 49*, 877−919.
31. Richard, J. P., and Frey, P. A. (1978) *J. Am. Chem. Soc. 100*, 7757−7758.
32. Dahms, A. S., Kanazawa, T., and Boyer, P. E. (1973) *J. Biol. Chem. 248*, 6592−6595.
33. Webb, M. R., and Trentham, D. R. (1981) *J. Biol. Chem. 256*, 4884−4887.
34. Cornelius, F. (1995) *Biochim. Biophys. Acta 1235*, 197−204.
35. Martin, D. W., and Sachs, J. R. (2000) in *Na/K-ATPase and Related ATPases* (Taniguchi, K., and Kaya, S., Eds.) pp 123−130, Elsevier, Amsterdam.
36. Hu, Y.-K., Eisses, J. F., and Kaplan, J. H. (2000) *J. Biol. Chem. 275*, 30734−30739.
37. Portillo, F. (2000) *Biochim. Biophys. Acta 1468*, 99−106.
38. Post, R. L., Toda, G., and Rogers, F. N. (1975) *J. Biol. Chem. 250*, 691−701.
39. Berberián, G., and Beaugé, L. (1991) in *The Sodium Pump: Recent Developments* (Kaplan, J. H., and De Weer, P., Eds.) pp 389−393, Rockefeller University Press, New York.
40. Heikinheimo, P., Lehtonen, J., Baykov, A., Lahti, R., Cooperman, B. S., and Goldman, A. (1996) *Structure 4*, 1491−1508.
41. Karlish, S. J. D., and Yates, D. W. (1978) *Biochim. Biophys. Acta 527*, 115−130.
42. Steinberg, M., and Karlish, S. J. D. (1989) *J. Biol. Chem. 264*, 2726−2734.
43. Faller, L. D., Kasho, V. N., Smirnova, I. N., Lin, S.-H., and Farley, R. A. (2000) in *Excerpta Medica International Congress Series 1207* (Taniguchi, K., and Kaya, S., Eds.) pp 389−396, Elsevier, Amsterdam.
44. Ridder, I. S., and Dijkstra, B. W. (1999) *Biochem. J. 339*, 223−226.
45. Smirnova, I. N., Lin, S.-H., and Faller, L. D. (1995) *Biochemistry 34*, 8657−8667.
46. Smirnova, I. N., and Faller, L. D. (1993) *Biochemistry 32*, 5967−5977.
47. Goldshleger, R., and Karlish, S. J. D. (1999) *J. Biol. Chem. 274*, 16213−16221.
48. Aravind, L., Galperin, M. Y., and Koonin, E. V. (1998) *Trends Biochem. Sci. 23*, 127−129.
49. Ovchinnikov, Y. A., Dzhandzugazyan, K. N., Lutsenko, S. V., Mustayev, A. A., and Modyanov, N. N. (1987) *FEBS Lett. 217*, 111−116.
50. Girardet, J.-L., Bally, I., Arlaud, G., and Dupont, Y. (1993) *Eur. J. Biochem. 217*, 225−231.
51. Pedersen, P. A., Jorgensen, J. R., and Jorgensen, P. L. (2000) *J. Biol. Chem. 275*, 37588−37595.
52. Vilsen, B., Andersen, J. P., and MacLennan, D. H. (1991) *J. Biol. Chem. 266*, 16157−16164.

BI010270+